Experimental study of magnetic bearing instability under supercritical CO_2 cooled MMR conditions

Do Kyu Kim, Seung Joon Baik, Jeong Ik Lee
Department of Nuclear and Quantum Engineering, KAIST, Daejeon, South Korea
Email: mike08@kaist.ac.kr , bsj227@kaist.ac.kr , jeongiklee@kaist.ac.kr

1. Introduction

The newly released IMO regulation forces the diesel engine on the container ship to be replaced to reduce CO_2 emission. Since the ship has limited space, the alternative engine should also be compact. A concept of fully modularized fast reactor with a supercritical CO_2 (S-CO_2) cooled direct Brayton cycle, namely Micro Modular Reactor (MMR), can potentially substitute the diesel engine by meeting those requirements. [1]

In case of MMR with 10MWe capacity, the magnetic bearing can be a proper choice for the turbomachinery. This can be readily supported by the previous research, which is also partially shown in Figure 1. MMR's bearing should have larger load capacity than gas foil bearing but should be free from contamination of CO_2. The magnetic bearing is appropriate for the MMR to support the rotor mass while no contamination problem is expected due to lubrication fluid.

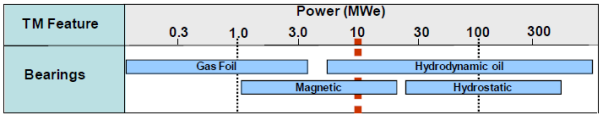

Figure 1. Bearing Options for S-CO_2 Brayton Cycles with various power scales [2]

There were several studies related to the bearing for S-CO_2 Brayton cycle application [4 &5]. However, an instability issue was repeatedly mentioned under high speed operation under S-CO_2 conditions of which orbit is described in figure 2. On the other hand, much higher speed operating in air condition does not have this issue (Figure 3). The instability induces the shaft imbalance to grow until the clearance between the shaft and stator disappears leading to crash. This instability issue was observed to be related to not only the operation speed but also the fluid conditions.

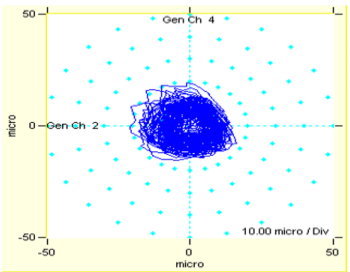

Figure 2. Shaft center orbit at 14,000rpm, 43°C , 78 bar under S-CO_2 condition

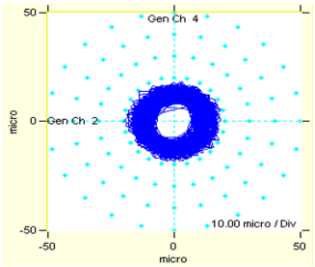

Figure 3. Shaft center orbit at 30,000rpm under air condition

Therefore, the interaction between S-CO_2 lubricating fluid and bearing is modeled with Reynolds equation, which describes the thin film flow. This model can calculates the pressure distribution around the shaft. From this model, the forces acting on the shaft in S-CO_2 conditions can be compared to the air conditions. In addition, the experimental results can be predicted by the calculation results.

In this paper, the developed S-CO_2 lubrication model is introduced. From the developed model, the magnetic bearing experiment is redesigned based on the calculation results. The experiment focuses on the verification of this model. This verification aims at finding the cause of instability and a method to resolve it. The modified layout of the experiment loop is suggested to achieve the experimental objectives.

2. Methods and Results

2.1 Magnetic bearing description

The magnetic bearing uses 8 electromagnets to apply the magnetic force to the rotor. The symmetrically located 8 electromagnets make possible to consider two axis of rotor separately. This is described in Figure 4. The inductive displacement sensor detects the clearance of the bearing. From the detected signal, the controller manipulates the magnetic force.

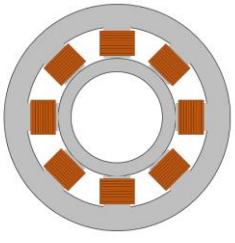

Figure 4. Cross Section of Radial Magnetic Bearing

The empty space is filled with the working fluid. In case of the Brayton cycle, the leaked fluid from the labyrinth seal cools the rotor as well.

Since the spaces between the electromagnets are too complex to formulate for the analysis and potentially a vortex can be generated to destabilize the shaft, the magnetic bearing is planned to have inner-coating to remove the geometry complexity. This is described in Figure 5.

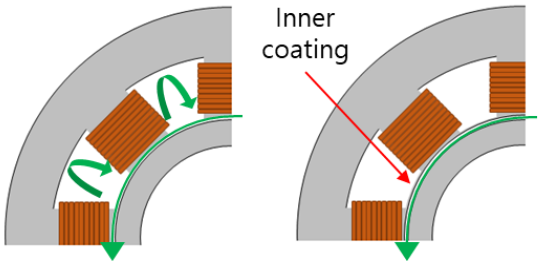

Figure 5. Schematic drawing of the bearing inner coating

2.2 Steady turbulent lubrication model of inner coated magnetic bearing

The experimental range of the model which will be introduced is described in Table 1. The experimental pressure range is from 1bar to 100bar. This is for the comparison between the high speed operation in air condition and the CO_2 condition with 1bar so the effect of the pressure and the fluid type, density can be compared. The temperature is near the CO_2's critical temperature which is also close to the room temperature. The rotational speed range is from 10000RPM to the 30000RPM. The reason is that the 15000RPM is the highest speed with CO_2 condition near critical point and the 30000RPM is the available speed in air condition. The eccentricity, ε is the ratio between the unbalanced length(e) and the averaged gap distance(c = R_2-R_1). The geometry is described in Figure 6. However, 0 value of eccentricity is meaningless. Eccentricity value near unity is an unstable condition.

Table 1. Operation condition range of the model

Supply temperature	20 ~ 40 °C
Supply pressure	1 ~ 100bar
Rotational speed	10000~30000 RPM
Eccentricity, ε	0.2~0.8

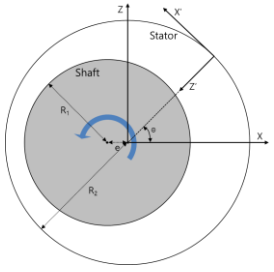

Figure 6. Geometry of the unbalanced shaft and the stator

Reynolds equation is a partial differential equation for thin film flow. The pressure distribution around the shaft with inner-coated magnetic bearing can be calculated with Reynolds equation. The Reynolds equation can be derived by substitution of the velocity profile from Navier-Stokes equation into the continuity equation. The equation is

$$\frac{\partial}{\partial X}\left(\frac{\rho h^3}{12\mu}\frac{\partial p}{\partial X}\right)+\frac{\partial}{\partial Y}\left(\frac{\rho h^3}{12\mu}\frac{\partial p}{\partial Y}\right) = \rho\frac{\partial h}{\partial t}+ h\frac{\partial \rho}{\partial t}+\frac{1}{2}\frac{\partial(\rho h u)}{\partial X}+\frac{1}{2}\frac{\partial(\rho h v)}{\partial Y} \quad [3]$$

(X : circumferential direction, Y : axial direction, Z : radial direction, t : time, w : radial velocity, u : circumferential velocity, h : gap, ρ : density, μ : viscosity. The X'-Z' frame is denoted as X-Z frame for convenience.)

The axial direction (Y axis) of the equation is negligible because the axial velocity is relatively small. In addition, the transient term is removed to consider the steady condition only. Therefore, the equation can be simplified.

$$\frac{\partial}{\partial X}\left(\frac{\rho h^3}{12\mu}\frac{\partial p}{\partial X}\right) = \frac{1}{2}\frac{\partial(\rho h u)}{\partial X}$$

The turbulence effect can be considered by the new coefficient k_x from the Ng-Pan model, which is k_x=12+K_x $(Re)^{nx}$ instead of the 12 in the left side of the equation ($Re = \rho c u/\mu$). The constants, K_x and n_x in the equation is described in table 2.

Table 2. Coefficient in Ng-Pan model

Reynolds' number	K_x	n_x
50,000<Re	0.0388	0.8
5000<Re<50000	0.0250	0.84
Re<5000	0.0039	1.06

The equation is numerically solved by finite difference method(FDM). The coordinate and thin film geometry for the FDM is described in Figure 7. The calculation flowchart is described in Figure 8.

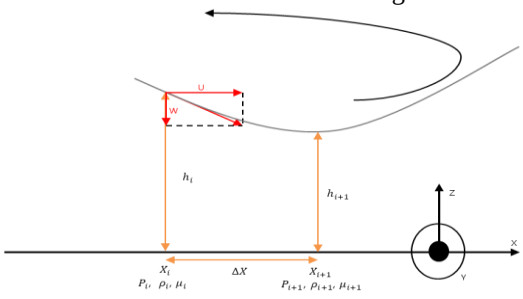

Figure 7. Coordinate description of Reynolds equation

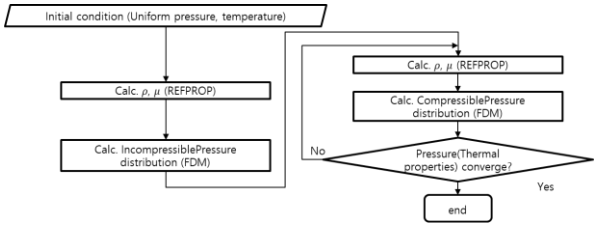

Figure 8. Flow chart of the pressure calculation

2.3 Analysis of the modeling

Before redesigning the experiment, the calculation results from this model should be analyzed. The comparison between 1bar and 80bar from the calculation results are described in Figure 9 to 10.

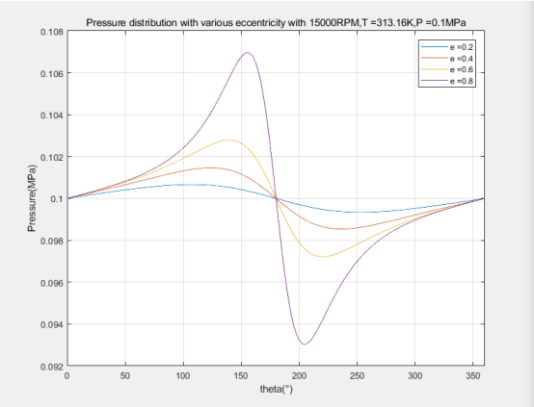

Figure 9. Pressure distribution with various eccentricity at 15000RPM, 40 °C and 1bar

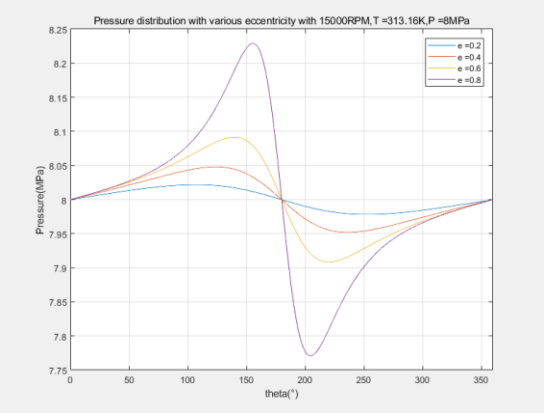

Figure 10. Pressure distribution with various eccentricity at 15000RPM, 40 °C and 80bar

From the pressure distribution, the force to the shaft can be calculated. The forces from the 1bar condition and 80bar condition is on the Tables 3 & 4.

Table 3. Forces on the shaft in 1bar CO_2 condition

	1 bar condition			
Eccentricity	ε = 0.2	ε = 0.4	ε = 0.6	ε = 0.8
Fx (N)	0.0061	0.0146	0.0507	0.2525
Fz (N)	-0.3551	-0.72	-1.13	-1.78

Table 4. Forces on the shaft in 80bar CO_2 condition

	80 bar condition			
Eccentricity	ε = 0.2	ε = 0.4	ε = 0.6	ε = 0.8
F_x (N)	0.268	0.661	1.588	11.798
F_z (N)	-11.68	-23.58	-37.07	-58.55

The F_x is the force which act in X direction and the F_z is the force which act in Z direction from Figure 4. The F_x assists to reduce the gap while the F_z doesn't.

From the table, the force in both direction under 1 bar condition is not significant. On the other hand, the F_z in 80 bar condition is quite large even in small eccentricity. In view of the eccentricity direction (e or X direction), this F_z is the asymmetrical element. So, from this results, it is concluded that the pressure is an important factor.

The other conditions such as supply temperature and rotational speed are planned to be analyzed with this model. From the physical model, The dominant factors which influence to the pressure distribution and the force will identified.

2.3 Redesigned experimental process

The experimental range is quite large. Therefore, the CO_2's thermal state should be controlled. S-CO_2 pressurizing experiment (S-CO_2PE) facility will be used for this purpose which is shown in Figure 11. From this facility, the temperature and pressure can be controlled.

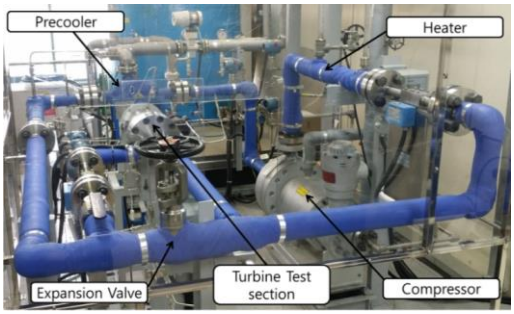

Figure 11. S-CO_2 power cycle demonstration facility (S-CO_2PE)

In addition, the magnetic bearing test rig is modified to verify the developed model. The test rig consists of the compressor and the magnetic bearing inside of it. The inverter will make the shaft rotate. The impeller is removed so only the thin film effect is expected to be dominant. That is the reason the magnetic bearing test rig's discharge port is blocked. So, the outlet is only the leakage port. It is shown in Figure 12.

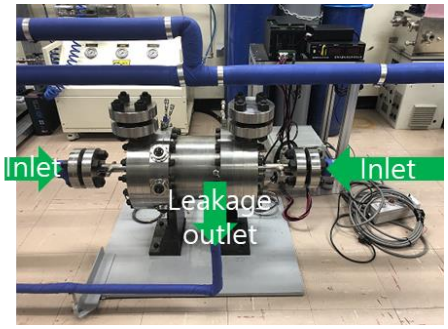

Figure 12. Magnetic bearing test rig

From this, the S-CO_2PE is upgraded as Figure 13 and 14. The booster pump is used to increase the system's pressure. Then, the pressure drop is compensated with the compressor.

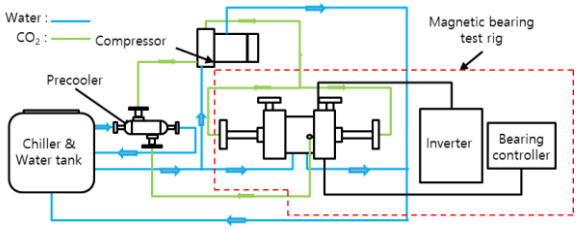

Figure 13. Layout of the bearing instability experiment

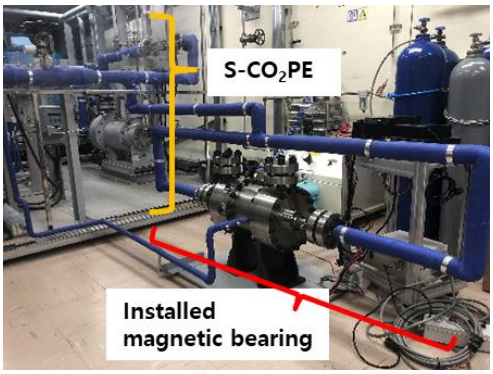

Figure 14. The magnetic bearing & compressor system for S-CO_2

Firstly, the magnetic bearing test without inner coating is planned under the conditions in Table 1. After this test, the bearing will have inner coating. The second test with inner coated magnetic bearing under the same conditions will be conducted. Finally, the third test will be conducted with an inner coating and no electromagnet control.

The experiment results will be analyzed with shaft center's trajectory. If the trajectory converges into a point, it can be said that it is stable. Even it did not converges into a point; it is also stable if the trajectory keeps an orbit with small fluctuation magnitude.

The second test can be compared to the first test. From this, the geometry complexity effect can be verified. The third test's results can be used to find the point where instability occurs. In addition, the tendency from the third results will be analyzed to verify the developed thin film model.

3. Conclusions

The effect of the unexpected flow will be analyzed from the comparison between the experiments that use electromagnets with and without inner coating. In addition, the experiments with inner coating and no electromagnet control will verify the modelling of the thin film fluid.

From the results, the demanded magnetic bearing performance can be suggested. Also, if the model is well validated, this model can be adapted to various S-CO_2 cycle systems.

Acknowledgement

This work was supported by the National Research Foundation of Korea (NRF) grant funded by the Korea government (MSIP) (2017M2B2B1071971)

REFERENCES

[1] Kim, S. G., Yu, H., Moon, J., Baik, S., Kim, Y., Jeong, Y. H., and Lee, J. I. (2017) A concept design of supercritical CO2 cooled SMR operating at isolated microgrid region. Int. J. Energy Res., 41: 512–525. doi: 10.1002/er.3633.

[2] Sienicki, James J., et al. "Scale dependencies of supercritical carbon dioxide Brayton cycle technologies and the optimal size for a next-step supercritical CO2 cycle demonstration." *SCO2 power cycle symposium*. 2011.

[3] Hamrock, Bernard J., Steven R. Schmid, and Bo O. Jacobson. *Fundamentals of fluid film lubrication*. CRC press, 2004.

[4] Dousti, Saeid, and Paul Allaire. "A compressible hydrodynamic analysis of journal bearings lubricated with supercritical carbon dioxide." *Proceeding of Supercritical CO2 Power Cycle Symposium, San Antonio, TX*. 2016.

[5] El-Shafei, A., and A. S. Dimitri. "Controlling journal bearing instability using active magnetic bearings." *Journal of Engineering for Gas Turbines and Power*132.1 (2010): 012502.